2002-01-0804

Damper Tuning with the use of a Seven Post Shaker Rig

Henri Kowalczyk

ARC Indianapolis-Reynard Motorsport

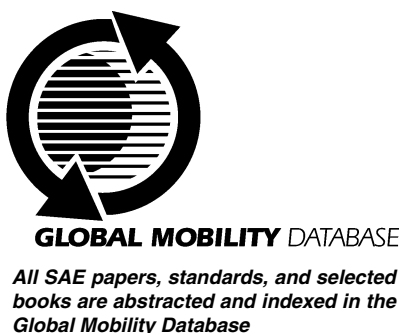The appearance of this ISSN code at the bottom of this page indicates SAE's consent that copies of the paper may be made for personal or internal use of specific clients. This consent is given on the condition, however, that the copier pay a per article copy fee through the Copyright Clearance Center, Inc. Operations Center, 222 Rosewood Drive, Danvers, MA 01923 for copying beyond that permitted by Sections 107 or 108 of the U.S. Copyright Law. This consent does not extend to other kinds of copying such as copying for general distribution, for advertising or promotional purposes, for creating new collective works, or for resale.

Quantity reprint rates can be obtained from the Customer Sales and Satisfaction Department.

To request permission to reprint a technical paper or permission to use copyrighted SAE publications in other works, contact the SAE Publications Group.

GLOBAL MOBILITY DATABASE

All SAE papers, standards, and selected books are abstracted and indexed in the Global Mobility Database

No part of this publication may be reproduced in any form, in an electronic retrieval system or otherwise, without the prior written permission of the publisher.

Positions and opinions advanced in this paper are those of the author(s) and not necessarily those of SAE. The author is solely responsible for the content of the paper. A process is available by which discussions will be printed with the paper if it is published in SAE Transactions. For permission to publish this paper in full or in part, contact the SAE Publications Group.

Persons wishing to submit papers to be considered for presentation or publication through SAE should send the manuscript or a 300 word abstract of a proposed manuscript to: Secretary, Engineering Meetings Board, SAE.

Printed in USA

2002-01-0804

Damper Tuning with the use of a Seven Post Shaker Rig

Henri Kowalczyk
ARC Indianapolis-Reynard Motorsport

ABSTRACT

Race sanctioning bodies have begun to drastically limit the number of days available to race teams for track testing in order to contain costs. Due to the limited amount of track time available it has become increasingly difficult to explore and exploit all of the possible changes that can be made to the car in order to improve its performance. Thus seven post testing is becoming more widely used by race teams to optimize their suspensions before arriving at the racetrack.

A seven post rig, as the name implies, comprises seven actuators. Four actuators are used to simulate the road inputs, while the other three actuators are used to simulate downforce and inertial loadings. The rig at the ARC is capable of reproducing various waveforms, including the capability of simulating track inputs. This paper describes modal testing of the car, where the modes of interest are the rigid body modes of the car: heave, pitch and roll. Future work will be concerned with results based on track simulation testing.

This paper describes how a seven post rig is used to optimize the suspension of a racecar. A quarter car model as well as a seven degree of freedom model with sprung mass freedoms of heave, pitch and roll, and vertical freedom of each unsprung mass, will be developed. Simulation results from the models will be used to illustrate the principles involved when tuning the suspension of a racecar. The results of the simulation will be related to the real world by showing results obtained from an actual seven post test of a Champcar.

INTRODUCTION

This paper describes the use of the seven post rig at the Auto Research Center (ARC) in Indianapolis to tune racecar suspensions. This facility has been in operation since early 1999 and is used by teams in varied motorsports categories ranging from open wheel race cars to stock cars. The ARC is a test facility consisting of a 50% rolling road wind tunnel and a seven post shaker. The seven post shaker is a unit manufactured by Servotest a leader in hydraulic test equipment. Servotest currently provides seven post shakers to most of the Formula 1 teams, as well as developing shakers for NVH and seismic testing. The Servotest system differs from many other shakers in that it is a true seven post system. Many shaker rigs are four post rigs that have been retrofitted with springs that allows for the application of a static aero loads. The main drawback to this method is that by attaching springs from the ground to the car the dynamics of the car are altered. The Servotest system on the other hand uses an active control system that is tuned to have a minimal impact on the dynamics of the car.

In the racing industry, damper tuning is seen as somewhat of an art. A force-velocity curve for a damper is a closely guarded secret. Damper engineers base these curves on years of experience of what a particular car "needs". Sometimes, when faced with a new situation a damper engineer will rely on theory based on quarter

car models. However, both of these methods have their shortcomings. Dampers based on experience are usually developed from driver feedback, thus they may or may not be transferable to other drivers or cars. Dampers based on simple linear models do not take advantage of non-linear capabilities of modern race dampers. In order to fully understand the non-linear dynamics of the vehicle, a non-linear model of both the car and dampers must be created. The time required to build and validate a model of this complexity is beyond the budgets of most race teams, thus the seven post rig is a useful tool for the teams to use in the optimization of their suspension.

In order to create meaningful test and analysis procedures for any system, its dynamics must be understood at least at a basic level. Simulations can be used to understand the dynamics of the system. These simulations can be useful in devising test methods and analysis procedures. At the ARC we have developed basic models of the vertical dynamics of the car in order to improve our testing methodology on the shaker rig. This paper describes the models, how they relate to the results observed on the rig, and finally the results of an actual test are described illustrating the validity of the findings of the models

The amount of data collected on the seven post rig can quickly become overwhelming; the models described in this paper have allowed us at the ARC to focus our analysis of the data generated by the seven post rig.

TEST PROCEDURE

Our current testing methodology consists of exciting the car with a swept sine where all the wheelpans are in phase (heave input) and minimizing the pitch and heave. We have been successful at using this form of optimization with varied forms of motorsports ranging from high downforce open wheel racecars to NASCAR Winston Cup cars.

The first step in the test procedure is to determine the inputs to the car. First the downforce levels are determined for a given cornering scenario. Then the wheelpan input amplitude is varied until the power

spectral density (PSD) of the damper displacement signals is similar to what is seen on the track. Since the input we are using is not the same as the input of the track surface, the PSDs will not exactly match. The aim is to not over or under excite the car. Once the input amplitude has been chosen the optimization can begin.

In its most basic form, the sole purpose of a suspension damper is to dissipate the energy stored in the spring. If this were its only purpose, then the optimization of the damper would be a relatively simple endeavor and would require only minimizing the resonant responses of the various modes. However, in an automobile suspension the damper serves a secondary purpose, controlling load transfer in transient maneuvers. How the load transfer is controlled by the damper is critical in giving the driver the feedback that he needs to drive the car at its limit. In cars with ground effects aerodynamics, the damper is also used to control the attitude of the car.

The tuning of the damper for the latter two requirements is guided by driver feedback. Tuning for the resonant responses can be carried out with the help of the seven post shaker. Although the end result is not necessarily a damper completely optimized to minimize resonant responses, these responses are usually reduced substantially through the course of a test session at the shaker.

MODEL DERIVATIONS

The following sections describe the vertical dynamics of a car, and show what can be done to optimize its response. These models illustrate the results that can be expected from the optimizing work done on the rig.

QUARTER CAR VEHICLE MODEL

Although a quarter car model is a very simplified representation of a car it is very popular in the literature of suspension research.[i] The reason for this popularity is that its simplicity allows for a closed form solution and thus leads to a greater understanding of the system. A quarter car

model has been developed and used to gain some insight into the behavior of a racecar suspension.

Figure 1 shows the geometry of the quarter car model derived in this section.
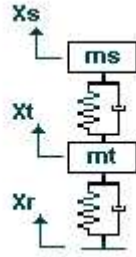

Figure 1 - Quarter Car Model

The quarter car model is used to study the behavior of the system around its equilibrium state; therefore, the displacements are taken to be zero at static equilibrium.

The variables of the model are defined as:

xs - Displacement of Sprung mass from equilibrium position
xt – Displacement of unsprun mass from equilibrium position
ks – suspension stiffness
cs – suspension damping
kt – tire vertical stiffness
cs – tire damping

The equations of motion can be derived using Lagrange's Equations for a holonomic system without external forces.

$$\frac{d}{dt}(\frac{\partial T}{\partial \dot{x}_s}) - (\frac{\partial T}{\partial x_s}) + \frac{\partial U}{\partial x_s} + \frac{\partial R}{\partial \dot{x}_s} = 0 \quad (1)$$

$$\frac{d}{dt}(\frac{\partial T}{\partial \dot{x}_t}) - (\frac{\partial T}{\partial x_t}) + \frac{\partial U}{\partial x_t} + \frac{\partial R}{\partial \dot{x}_t} = 0 \quad (2)$$

The kinetic energy of the system is given by eqn 3.

$$T = \frac{1}{2}m_s \dot{x}_s^{\,2} + \frac{1}{2}m_t \dot{x}_t^{\,2} \quad (3)$$

The effects of the suspension geometry are accounted for in the suspension stiffness coefficient. This is an average vertical rate which accounts for any rising rate characteristics of the suspension. The potential energy of the system is given by eqn 4

$$U = \frac{1}{2}k_s(x_t - x_s)^2 + \frac{1}{2}k_t(x_r - x_t)^2 \quad (4)$$

The non-linear characteristics of the damper have been lumped into the damping coefficient. This includes the effects of suspension geometry as well as the differences in bump and rebound damping. The Rayleigh dissipation function of the dampers and damping of the tire is given by eqn 5.

$$R = \frac{1}{2}c_s(\dot{x}_t - \dot{x}_s)^2 + \frac{1}{2}c_t(\dot{x}_r - \dot{x}_t)^2 \quad (5)$$

Substituting eqns 3,4 and 5 into 1 and 2 yields the equations of motion for the quarter car.

$$m_s \ddot{x}_s - c_s(\dot{x}_t - \dot{x}_s) - k_s(x_t - x_s) = 0 \quad (6)$$

$$m_t \ddot{x}_t + c_s(\dot{x}_t - \dot{x}_s) - c_t(\dot{x}_r - \dot{x}_t)$$
$$+ k_s(x_t - x_s) - k_t(x_r - x_t) = 0 \quad (7)$$

Root Locus Analysis of Damping Coefficient

The root locus procedure can be used to study the effects of a parameter on the response of the system. Here, the effect of varying the damping coefficient is studied. Tire damping has been neglected in the subsequent analysis of the quarter car in order to simplify the mathematics; this is a valid assumption since tire damping is much less than that provided by the dampers, and it decreases with rolling speed.[ii]

Figure 2 shows the root locus for a quarter car model of a typical Champcar in street

course configuration. The parameters used for the root locus are for a front corner and are shown in Table 1 in the appendix.
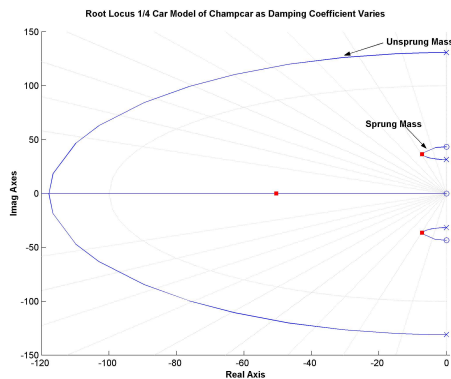

Figure 2

The root locus shows the effects of varying the damping coefficient of the quarter car model. The pole trajectory for the unsprung mass shows that adequate damping, a damping ratio of 1, can be achieved by increasing the damping coefficient. This occurs when the pole related to the unsprung mass motion is on the real axis. The markers on figure 2 show the damping coefficient of 49 lb/(in/s) [8581 N/(m/s)] that results in well damped unsprung mass mode (the marker is on the real axis), however, this amount of damping only results in a damping ratio of about .2 for the sprung mass. Conventional wisdom would indicate that increasing the damping coefficient would improve the situation and dampen the body mode. In fact the opposite results. The root locus analysis shows that increasing the damping coefficient will decrease the damping of the sprung mass mode.

The reason for this limitation is that the stiffness of the tire is the same order of magnitude as the spring stiffness. Increasing the damper stiffness by increasing the damping coefficient will limit the movement of the suspension, and will increase the deflection of the tire, so that the sprung mass then bounces on the tire. The manifestation of this phenomenon is known in the racing community as locking the shock. In contrast to this situation we can examine a passenger car suspension,

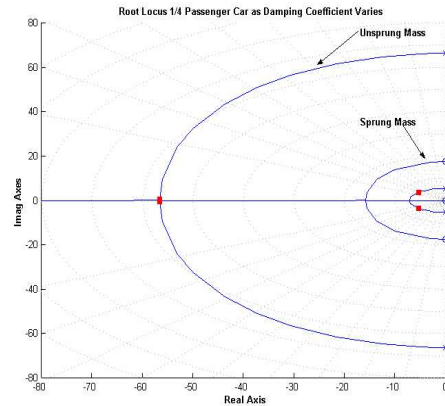where the tire stiffness is much higher than the suspension stiffness.

Figure 3

Figure 3 shows the root locus for a typical road car suspension, the parameters used are shown in Table 2 in the appendix. The root locus shows that the damping ratio for both modes moves closely together as the damping coefficient is increased. The square marker shows the current roots for a damping value of 65 lb/(in/s) [11383 N/(m/s)]. For this amount of damping the unsprung mass mode is overdamped, the pole is on the real axis, and the sprung mass mode is almost as well damped with a .8 damping ratio. Thus the damper dampens both modes relatively equally.

Unlike the racecar, the tires of a passenger car are quite stiffer than the suspension springs, thus increasing the damping does not increase the displacement of the tire substantially. However, this brings about other difficulties, since increasing the damping coefficient to dampen the sprung and unsprung masses will result in increased transmissibility of road vibrations to the passenger compartment.

SEVEN DEGREE OF FREEDOM (DOF) CAR MODEL

Although the heave response of the car can be easily understood with the quarter car model, a seven DOF model shows the interactions of the different modes. The car is modeled as an independently sprung, rigid body with pitch and roll motions about

its principal axes. The suspension geometry effects are neglected, except for motion ratio considerations. The motion ratio is used to generate an equivalent vertical spring stiffness and damping at the wheel. Figure 4 shows the geometry of this model.
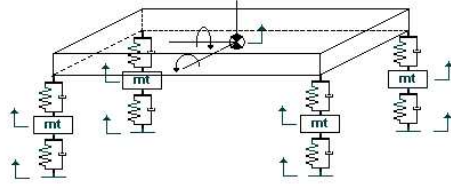

Figure 4 –Seven DOF Car Model

The variables of the model are defined as:

x_s – vertical displacement of sprung mass
Θ_p – pitch angle of sprung mass
Θ_r – roll angle of sprung mass
x_{fl} – vertical displacement of front left tire
x_{fr} – vertical displacement of front right tire
x_{rl} – vertical displacement of rear left tire
x_{rr} – vertical displacement of rear right tire
y_{fl} – vertical input at front left tire
y_{fr} – vertical input at front right tire
y_{rl} – vertical input at rear left tire
y_{rr} – vertical input at rear right tire
m_s – sprung mass
I_p – pitch inertia
I_r – roll inertia
m_{tfl} – front left tire mass
m_{tfr} – front right tire mass
m_{trl} – rear left tire mass
m_{trr} – rear right tire mass
k_{fl} – front left suspension stiffness
k_{fr} – front right suspension stiffness
k_{rl} – rear left suspension stiffness
k_{rr} – rear right suspension stiffness
c_{fl} – front left damping coefficient
c_{fr} – front right damping coefficient
c_{rl} – rear left damping coefficient
c_{rr} – rear right damping coefficient
k_{tfl} – front left tire stiffness
k_{tfr} – front right tire stiffness
k_{trl} – rear left tire stiffness
k_{trr} – rear right tire stiffness
c_{tfl} – front left tire damping coefficient
c_{tfr} – front right tire damping coefficient
c_{trl} – rear left tire damping coefficient
c_{trr} – rear right tire damping coefficient
a – distance from cg to front axle
b – distance from cg to rear axle
tf – front track width

tr – rear track width

Again we use Lagrange's Equations to derive the equations of motion.

The kinetic energy of the system consists of the translational energy of the masses as well as the rotational kinetic energy of roll and pitch of the sprung mass. The kinetic energy is given by eqn 8.

$$
\begin{aligned}
T = &\frac{1}{2}m_s\,\dot{x}_s^2 + \frac{1}{2}I_p\,\dot{\Theta}_p^2 + \frac{1}{2}I_r\,\dot{\Theta}_r^2 + \frac{1}{2}m_{tfl}\,\dot{x}_{fl}^2 \\
&+\frac{1}{2}m_{tfr}\,\dot{x}_{fr}^2 + \frac{1}{2}m_{trl}\,\dot{x}_{rl}^2 + \frac{1}{2}m_{trr}\,\dot{x}_{rr}^2
\end{aligned}
\tag{8}
$$

The potential energy of the system is given by eqn 9.

$$
\begin{aligned}
U = &\frac{1}{2}k_{fr}\left(x_{fr} - a\Theta_p - x_s + \frac{tf}{2}\Theta_r\right)^2 \\
&+\frac{1}{2}k_{fl}\left(x_{fl} - a\Theta_p - x_s - \frac{tf}{2}\Theta_r\right)^2 \\
&+\frac{1}{2}k_{rr}\left(x_{rr} + b\Theta_p - x_s + \frac{tr}{2}\Theta_r\right)^2 \\
&+\frac{1}{2}k_{rl}\left(x_{rl} + b\Theta_p - x_s - \frac{tr}{2}\Theta_r\right)^2 \\
&+\frac{1}{2}k_{tfr}\left(y_{fr} - x_{fr}\right)^2 + \frac{1}{2}k_{tfl}\left(y_{fl} - x_{fl}\right)^2 \\
&+\frac{1}{2}k_{trr}\left(y_{rr} - x_{rr}\right)^2 + \frac{1}{2}k_{trl}\left(y_{rl} - x_{rl}\right)^2
\end{aligned}
\tag{9}
$$

The Rayleigh dissipation function of the dampers and damping in the tires is given by eqn **10**.

$$
\begin{aligned}
R = &\frac{1}{2}c_{fr}\left(\dot{x}_{fr} - a\dot{\Theta}_p - \dot{x}_s + \frac{tf}{2}\dot{\Theta}_r\right)^2 \\
&+\frac{1}{2}c_{fl}\left(\dot{x}_{fl} - a\dot{\Theta}_p - \dot{x}_s - \frac{tf}{2}\dot{\Theta}_r\right)^2 \\
&+\frac{1}{2}c_{rr}\left(\dot{x}_{rr} + b\dot{\Theta}_p - \dot{x}_s + \frac{tr}{2}\dot{\Theta}_r\right)^2 \\
&+\frac{1}{2}c_{rl}\left(\dot{x}_{rl} + b\dot{\Theta}_p - \dot{x}_s - \frac{tr}{2}\dot{\Theta}_r\right)^2 \\
&+\frac{1}{2}c_{tfr}\left(\dot{y}_{fr} - \dot{x}_{fr}\right)^2 + \frac{1}{2}c_{tfl}\left(\dot{y}_{fl} - \dot{x}_{fl}\right)^2 \\
&+\frac{1}{2}k_{trr}\left(\dot{y}_{rr} - \dot{x}_{rr}\right)^2 + \frac{1}{2}k_{trl}\left(\dot{y}_{rl} - \dot{x}_{rl}\right)^2
\end{aligned}
\tag{10}
$$

Substituting into Lagrange's equations results in the equations of motion for the 7 DOF model. The equations of motion can be found in Appendix B.

SEVEN POST RIG DATA ANALYSIS

The rig instrumentation can include up to 40 channels of vehicle data and it is easy to become overwhelmed with the analysis. In order to simplify the analysis, only a few parameters are tracked, and when further analysis is warranted the remaining channels are analyzed. Most of the data reduction occurs in the frequency domain. Computer software has been written in Matlab using the signal processing toolbox in order to automate the analysis procedure. The analysis consists of obtaining the frequency response function (FRF) of the major modes of the vehicle; specifically the heave, pitch and roll modes of the sprung mass as well as the vertical modes of the unsprung mass.

This section discusses how these FRF's are obtained. In the subsequent section the equivalent responses will be obtained for the 7 DOF model.

The FRF is given by H(f) in eqn 11

$$Y(f) = H(f) * X(f) \qquad (11)$$

where Y(f) is the system response and X(f) is the input signal, both of these signals are measured and thus eqn 11 can be solved for H(f). Using the transfer function estimate function (TFE) in Matlab's signal processing toolbox solves for H(f). This function divides the data into overlapping blocks, windows the data with a Hanning window to reduce leakage and finally forms the transfer function using the H1 estimate of the FRF. The H1 estimate is given by eqn 12

$$H_1 = \frac{G_{XY}(f)}{G_{XX}(f)} \qquad (12)$$

where $G_{xy}(f)$ is the cross-spectrum of X and Y and $G_{xx}(f)$ is the auto-spectrum of X. The H_1 estimate gives the best estimate of the transfer function if the noise only contaminates the measurements of the output Y of the system.[iii] In the case of the seven post rig, the input signals are created by the control system so therefore can be assumed to be noise free.

For the discussions in this case study we are only concerned with heave and pitch motions since the car is symmetric in the roll axis, thus only two accelerometers are sufficient to describe the motions of the car. One accelerometer is placed along the centerline of the car on the front axle line, and another one is placed on the centerline along the rear axle line. From the geometry of the locations of the accelerometers we can define the following heave and pitch given by eqns 13 - 14

$$Heave = \frac{\dfrac{b * FrontAccel + a * RearAccel}{a+b}}{InputAcceleration} \qquad (13)$$

$$Pitch = \frac{\dfrac{FrontAccel - RearAccel}{a+b}}{InputAcceleration} \qquad (14)$$

Eqn 16, the contact patch load magnification transfer function, shows how well the tire is kept in contact with the road. A load cell in each wheelpan measures the vertical force at each contact patch. Since the longitudinal and lateral force generation of the tire is proportional to the vertical load, minimizing the variation of the contact patch load leads to a more constant lateral and longitudinal force generation. Looking at this graph for the front and rear pairs is useful when making adjustments to improve particular areas of handling. For example, to improve traction of the rear wheels the contact load variation at the rear would need to be minimized.

$$ContactPatchLoadMagnification = \frac{ContactLoad}{InputAccel} \qquad (16)$$

Ideally, an optimized car would have the lowest possible FRF's for all of the above. The results of the simulations will show that all of the FRF's cannot be minimized concurrently.

7 DOF CAR MODEL DATA ANALYSIS

The equations of motion of the 7-DOF car model can be integrated numerically to find the response of the car to a given input. A MATLAB program has been written in order to accomplish this. The input to the simulation can be the same as that used on the seven post rig, thus allowing for a direct comparison of the results. The outputs of the simulation are the time domain responses of each of the degrees of freedom of the model. The time domain outputs of the simulation are used as inputs to the transfer function estimate function (TFE) to find the FRF's.

The rigid body motions of the model are given by the displacement of the sprung mass, X_s, the pitch angle, $\bullet_p$. The FRF's are then found using eqns 17 - 18

$$Heave = \frac{X_s}{Y_{fl}} \quad (17)$$

$$Pitch = \frac{\Theta_p}{Y_{fl}} \quad (18)$$

Since the input is a pure heave displacement all four wheel displacements will be the same and thus it is sufficient to use the displacement of one of the corners, in this case we chose the front left wheelpam, Y_{fl}.

ROAD INPUT MODEL

The road input used for modal testing is a swept sine of constant maximum velocity. The amplitude of the swept sine is chosen so that the damper response on the rig is similar to that seen at the track. The power spectral density (PSD) of damper velocity data logged at the track is the target response. The road amplitude is then varied until a suitable match is found. This process occurs offline and requires the user to make a judgment as to when a suitable input has been found. Based on the experience of the ARC staff this procedure will usually require only a few iterations to produce a reasonable input.

The constant maximum velocity input is based on the properties of real road profiles. Wong[iv] gives the PSD of displacement of a road profile as:

$$S(\Omega) = C_{sp}\Omega^{-N} \quad (20)$$

where Ω is the spatial frequency in cycles per meter or per foot, and C_{sp} and N are tabulated for different surfaces. The value N can range from 1 to about 4 depending on the road surface characteristics.

If we assume that the car is travelling over the road at a constant velocity V, then the PSD of the road in Hz can be found by substituting:

$$\Omega = \frac{f(Hz)}{V(m/s)} \quad (21)$$

which results in a PSD in the frequency domain of:

$$S(f) = C_{sp}(f/V)^{-N} \quad (22)$$

Recall that to find the velocity PSD from the displacement PSD it is only necessary to multiply by the frequency in the frequency domain, thus if we assume N=1 the velocity PSD becomes:

$$S_V(f) = C_{sp}V \quad (23)$$

which is independent of frequency and our assumption of a constant maximum amplitude velocity swept sine is valid.

SIMULATION RESULTS FOR 7 DOF CAR MODEL

It is useful to study the results of a linear simulation to gain insight into the dynamics of the system, although clearly the simulations are limited since the real car includes many non-linear elements. The linear simulations can be used to give a qualitative representation of what happens when changes are made to damping levels; figure 5 shows an example where a simulation has been run to study relative damping levels. In this example, the front

and rear damping levels are varied and the effects on the maximum of the heave and pitch frequency response function are plotted in a contour plot. The y-axis is the front damping coefficient in lb/in/s and the x axis is the rear damping coefficient also in lb/in/s. The parameters used for the results of figure 5 are shown in Table 1 in the appendix. The parameters correspond to the car tested in the case study section. Although the results are for a single setup of springs, the trend is representative for the range of springs commonly used in Champcars.

The contours of maximum heave response show the lowest response to be roughly 1.75. Recall from the root locus study that the heave response of the car is limited by the tire stiffness. Therefore it is not surprising that adjusting the damping cannot further reduce the heave response.

Another result which is evident in the contour plot is the necessity to strike a compromise between heave and pitch response. Figure 5 shows that it is not possible to achieve minimum pitch and minimum heave concurrently. In order to minimize the pitch response of the car it is necessary to increase the rear damping, however, this is detrimental to heave response. Thus a judgment call must be made as to which response is most important.
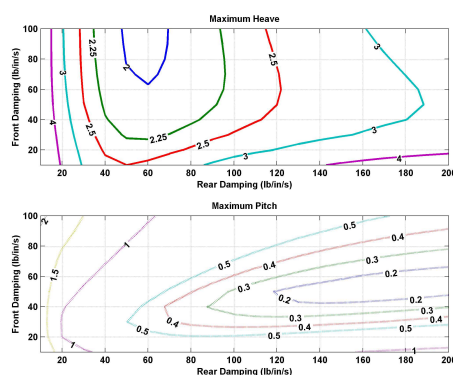

Figure 5

LIMITATIONS OF LINEAR MODELS

Although the 7 DOF model is a vast improvement over the ¼ car model, it is still a simplified linear model. The benefit of this model is that it gives a qualitative picture of what effect relative damping levels will have on the dynamics of the car. Another benefit is in the study of parameters such as CG position, pitch inertia, or wheelbase. These changes are changes that are routinely made to Champcars by ballast and suspension geometry adjustments. The linear model gives a quick indication as to the merit of the proposed changes.

The linear model has been used mainly to understand the dynamics of the car. It shows the realistic limits to which the resonances can be reduced, thus we do not waste time needlessly searching for better and better responses.

The main limitation of the model is that it does not provide for non-linear dampers. Race dampers are fully adjustable in compression and rebound as well as low and high speed ranges. Race teams do not have the resources to create fully non-linear simulations, thus the non-linear effects are better studied using the seven post shaker.

CASE STUDY

This section describes the optimization procedure used on a Champcar and ties it to the results of the earlier sections of this paper.

As discussed in previous sections, the input used to excite the car is a pure heave input. The input to the wheelpans is a swept sine starting a .5 Hz and stopping at 20 Hz, with a constant maximum velocity of 100 mm/s. The constant maximum velocity is equivalent to assuming N=1 in the road input model presented earlier.

Recall that the root locus analysis shows that wheelhop is not a major concern for a Champcar, thus the analysis of the optimization is mainly centered on optimizing the sprung mass modes, heave and pitch. Depending on the car tested, roll is also considered, however, for a Champcar the roll response is very small and in any case this data refers to a symmetric setup for a street course which does not exhibit a roll component when excited in heave.

As the results of the previous section showed, heave and pitch cannot be minimized concurrently, thus we tend to concentrate on minimizing the pitch response. This is consistent with results published by other authors, such as for example Kasprzak & Floyd[v]. The benefit of reducing pitch response appears to be twofold. First for cars which have aerodynamic pitch sensitivity limiting pitch will result in a more stable aerodynamic platform by reducing the movement of the aerodynamic center of pressure. Second, there is also a gain of mechanical grip and stability which is reported by the drivers. To understand these results, consider what happens when the car pitches nose down; the front spring will be compressed, and thus the vertical load at the front tires will increase. This will increase the lateral force of the front tires. However, at the same time the rear rises and thus lowers the vertical load at the rear tires, lowering the lateral force. Since a pair of tires equally loaded will produce the greatest amount of lateral force for a given amount of total vertical load it is easy to see that minimizing the pitch response will result in the overall greatest lateral force. Also, if the car is oscillating in pitch, the mechanical center of pressure will move which the driver considers an unstable situation.

Figures 6 & 7 are indicative of the results obtained from a session at the seven post shaker rig. Figure 6 shows the heave response of the car. Notice that there has been a slight increase (11%) in heave response, signaling a slight loss of control of the heave mode. However, figure 7 shows a large improvement in the pitch response of the car (43%). Unfortunately due to sensitive nature of the information provided by damper curves we cannot publish the actual damper curves that were used to arrive at these results. However, the subsequent discussion using the linear model should make the salient points of the optimization evident.
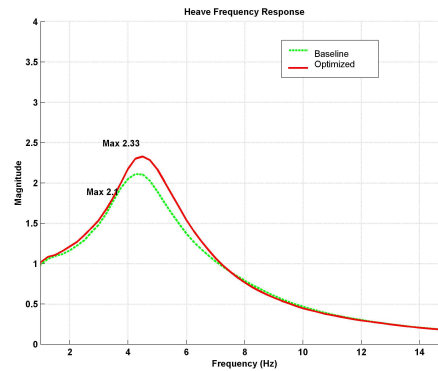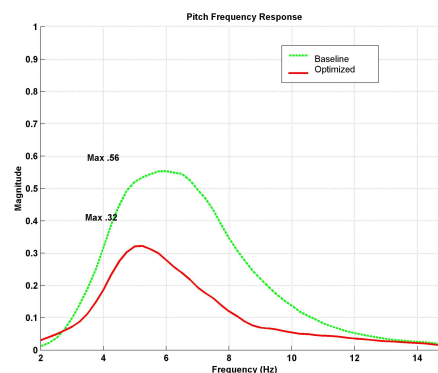

Figure 6

Figure 7

Figure 8 shows the same results as Figure 5 but with a limited number of contours to show more clearly the operating condition for this case study. The plot was generated by using the parameters for the car discussed in this section. The arrow on figure 8 shows the direction the direction that needs to be taken in order to improve the pitch response of the car, less front damping and more rear damping. For this case we lowered the front rebound damping slightly and increased the rear rebound damping, this produced the optimized setup of figures 6 & 7. Note that our simulation was not used to find out absolute values of damping required, but instead it served as a guide as to what adjustments should be made to the damping levels in order to improve the response of the car. The final damping adjustments made to the car are based on the rig results and in consultation with the race engineer. The race engineer provides the feedback of what can be expected by changing certain characteristics of the damping curve. In this case it was felt

that increasing the rear rebound damping would be the most effective way of increasing the rear damping levels; thus the final result is a combination of shaker rig improvements while maintaining the correct feel of the dampers for the track.

It is interesting to note that although the car has many non-linear elements as mentioned in previous sections, it exhibits FRF's which appear linear about its operating point. In other words, once the excitation level and downforce level has been fixed the response is quite linear. For example, although the motion ratio increases quite substantially for these cars none of the stiffening spring response characteristics can be seen in the FRFs.
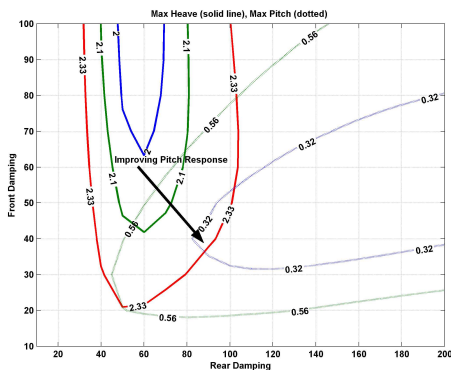

Figure 8

SUMMARY

The seven post rig has been a very useful tool in the tuning of race car suspensions. It has been used to successfully optimize the dampers on many different types of cars ranging from powerful ground effects cars such as Champcars to NASCAR Winston Cup cars. The models described in this paper show the dynamics of the car and how they are related to the optimization process that is carried out on the shaker rig. The use of simulations has allowed us to better understand the dynamics of the vehicles and it has enabled us to make strategic decisions on the test procedure and analysis on the seven post shaker. The simulations presented in this paper show some of the limitations that are present when attempting to optimize the response of the car by tuning of the dampers. Although

the simulations are simple linear models they are sufficient to understand the dynamics of the vehicles that we have tested. Producing fully non-linear simulations is beyond the capability and resources of most race teams, the use of the seven post shaker rig eliminates the need for such simulations.

CONTACT

Henri Kowalczyk
Vehicle Dynamics Engineer
Auto Research Center-Reynard Motorsport
4012 Championship Drive
Indianapolis, IN 46268
(317)-291-8600 xt58
hkowalczyk@reynardna.com

APPENDIX A – CAR PARAMETERS

Due to the confidential nature of racing, the parameters shown in Table 1 are not exact values, instead they are representative values of a present day Champcar race car.

Table 1

Champcar Street Course Parameters	
Front Suspension Stiffness	251174 N/m
Rear Suspension Stiffness	97533 N/m
Front Tire Stiffness	315234 N/m
Rear Tire Stiffness	332747 N/m
Sprung Mass	690 kg
Front Unsprung Mass	35 kg
Rear Unsprung Mass	40 kg
Pitch Inertia	520 kg m^2

Roll Inertia	25 kg m^2
CG to Front Axle	1.7 m
CG to Rear Axle	1.4 m

Table 2

Typical Passenger Quarter Car Parameters[vi]	
Suspension Stiffness	39000 N/m
Tire Stiffness	400000 N/m
Sprung Mass	1200 kg
Unsprung Mass	100 kg

APPENDIX B - SEVEN DOF EQUATIONS OF MOTION

$$m_s \, \ddot{x}_s - c_{fr} \, (\dot{x}_{fr} - a \, \dot{\Theta}_p - \dot{x}_s + \frac{tf}{2} \dot{\Theta}_r)$$

$$- c_{fl} \, (\dot{x}_{fl} - a \, \dot{\Theta}_p - \dot{x}_s - \frac{tf}{2} \dot{\Theta}_r)$$

$$- c_{rr} \, (\dot{x}_{rr} + b \, \dot{\Theta}_p - \dot{x}_s + \frac{tr}{2} \dot{\Theta}_r)$$

$$- c_{rl} \, (\dot{x}_{rl} + b \, \dot{\Theta}_p - \dot{x}_s - \frac{tr}{2} \dot{\Theta}_r)$$

$$- k_{fr} \, (x_{fr} - a \, \Theta_p - x_s + \frac{tf}{2} \Theta_r)$$

$$- k_{fl} \, (x_{fl} - a \, \Theta_p - x_s - \frac{tf}{2} \Theta_r)$$

$$- k_{rr} \, (x_{rr} + b \, \Theta_p - x_s + \frac{tr}{2} \Theta_r)$$

$$- k_{rl} \, (x_{rl} + b \, \Theta_p - x_s - \frac{tr}{2} \Theta_r) = 0$$

$$I_p \, \ddot{\Theta}_p - a \cdot c_{fr} \, (\dot{x}_{fr} - a \, \dot{\Theta}_p - \dot{x}_s + \frac{tf}{2} \dot{\Theta}_r)$$

$$- a \cdot c_{fl} \, (\dot{x}_{fl} - a \, \dot{\Theta}_p - \dot{x}_s - \frac{tf}{2} \dot{\Theta}_r)$$

$$- b \cdot c_{rr} \, (\dot{x}_{rr} + b \, \dot{\Theta}_p - \dot{x}_s + \frac{tr}{2} \dot{\Theta}_r)$$

$$- b \cdot c_{rl} \, (\dot{x}_{rl} + b \, \dot{\Theta}_p - \dot{x}_s - \frac{tr}{2} \dot{\Theta}_r)$$

$$- a \cdot k_{fr} \, (x_{fr} - a \, \Theta_p - x_s + \frac{tf}{2} \Theta_r)$$

$$- a \cdot k_{fl} \, (x_{fl} - a \, \Theta_p - x_s - \frac{tf}{2} \Theta_r)$$

$$- b \cdot k_{rr} \, (x_{rr} + b \, \Theta_p - x_s + \frac{tr}{2} \Theta_r)$$

$$- b \cdot k_{rl} \, (x_{rl} + b \, \Theta_p - x_s - \frac{tr}{2} \Theta_r) = 0$$

$$I_r \, \ddot{\Theta}_r + \frac{tf}{2} \cdot c_{fr} \, (\dot{x}_{fr} - a \, \dot{\Theta}_p - \dot{x}_s + \frac{tf}{2} \dot{\Theta}_r)$$

$$- \frac{tf}{2} \cdot c_{fl} \, (\dot{x}_{fl} - a \, \dot{\Theta}_p - \dot{x}_s - \frac{tf}{2} \dot{\Theta}_r)$$

$$+ \frac{tr}{2} \cdot c_{rr} \, (\dot{x}_{rr} + b \, \dot{\Theta}_p - \dot{x}_s + \frac{tr}{2} \dot{\Theta}_r)$$

$$- \frac{tr}{2} \cdot c_{rl} \, (\dot{x}_{rl} + b \, \dot{\Theta}_p - \dot{x}_s - \frac{tr}{2} \dot{\Theta}_r)$$

$$+ \frac{tf}{2} \cdot k_{fr} \, (x_{fr} - a \, \Theta_p - x_s + \frac{tf}{2} \Theta_r)$$

$$- \frac{tf}{2} \cdot k_{fl} \, (x_{fl} - a \, \Theta_p - x_s - \frac{tf}{2} \Theta_r)$$

$$+ \frac{tr}{2} \cdot k_{rr} \, (x_{rr} + b \, \Theta_p - x_s + \frac{tr}{2} \Theta_r)$$

$$- \frac{tr}{2} \cdot k_{rl} \, (x_{rl} + b \, \Theta_p - x_s - \frac{tr}{2} \Theta_r) = 0$$

$$m_{tfl} \, \ddot{x}_{fl} + c_{fl} \, (\dot{x}_{fl} - a \, \dot{\Theta}_p - \dot{x}_s - \frac{tf}{2} \dot{\Theta}_r)$$

$$- c_{tfl} \, (\dot{y}_{fl} - \dot{x}_{fl})$$

$$+ k_{fl} \, (x_{fl} - a \, \Theta_p - x_s - \frac{tf}{2} \Theta_r)$$

$$- k_{tfl} \, (y_{fl} - x_{fl}) = 0$$

$$m_{tfr}\, \ddot{x}_{fr} + c_{fr}\, (\dot{x}_{fr} - a\,\dot{\Theta}_p - \dot{x}_s + \frac{tf}{2}\,\dot{\Theta}_r\,)$$

$$-\, c_{tfr}\, (\dot{y}_{fr} - \dot{x}_{fr}\,)$$

$$+\, k_{fr}\, (x_{fr} - a\,\Theta_p - x_s + \frac{tf}{2}\,\Theta_r\,)$$

$$-\, k_{tfr}\, (y_{fr} - x_{fr}\,) = 0$$

$$m_{trl}\, \ddot{x}_{rl} + c_{rl}\, (\dot{x}_{rl} + b\,\dot{\Theta}_p - \dot{x}_s - \frac{tr}{2}\,\dot{\Theta}_r\,)$$

$$-\, c_{trl}\, (\dot{y}_{rl} - \dot{x}_{rl}\,)$$

$$+\, k_{rl}\, (x_{rl} + b\,\Theta_p - x_s - \frac{tr}{2}\,\Theta_r\,)$$

$$-\, k_{trl}\, (y_{rl} - x_{rl}\,) = 0$$

$$m_{trr}\, \ddot{x}_{rr} + c_{rr}\, (\dot{x}_{rr} + b\,\dot{\Theta}_p - \dot{x}_s + \frac{tr}{2}\,\dot{\Theta}_r\,)$$

$$-\, c_{trr}\, (\dot{y}_{rr} - \dot{x}_{rr}\,)$$

$$+\, k_{rr}\, (x_{rr} + b\,\Theta_p - x_s + \frac{tr}{2}\,\Theta_r\,)$$

$$-\, k_{trr}\, (y_{rr} - x_{rr}\,) = 0$$

[i] Chalasani, R. M., "Ride Performance Potential of Active Suspension Systems-Part 1:Simplified Analysis Based on a Quarter Car Model". ASME Symposium on Simulation of Ground Vehicles and Transport Systems CA, 1986

[ii] Genta, G., "Motor Vehicle Dynamics: Modeling and Simulation"

[iii] Randall, R.B., "Frequency Analysis", 3rd ed., Brüel & Kjaer 1987

[iv] Wong, J.Y., "Theory of Ground Vehicles", 2nd ed., Wiley Interscience 1993

[v] Kasprzak, J.L., Floyd, R. S., "Use of Simulation to Tune Race Car Dampers" SAE 942504

[vi] Classnotes ME653:Vehicle Dynamics, Dr. E.H. Law, Clemson University – Motorsports Engineering Program